Post-Processing of Air Entrainment on NASIR Flow Solver Results for Skimming Flow over Stepped Chutes

SAEED REZA SABBAGH-YAZDI*, ROSITA SAFAHIEH**

Associate Professor, Department of Civil Engineering
K.N.TOOSI University of Technology
Civil Engineering Department,
KN Toosi University of Technology,
No.1346 Valiasr
Street, 19697- Tehran
IRAN

and

NIKOS E. MASTORAKIS
Military Insitutes of University Education (ASEI)
Hellenic Naval Academy
Terma Chatzikyriakou 18539,
Piraues, GREECE

Abstract: - Air entrainment plays an important role in the reduction of cavitations risk potential in chutes and spillways. The advantages of stepped spillways over conventional smooth spillways, the air entrainment phenomenon, and the flow regimes occurring on stepped chutes have been reviewed. Then the numerical analysis of skimming flow using shallow water equations in inclined coordinate system is described. The numerical computations of air entrainment in the skimming flow over stepped spillways are performed in two stages. In the first stage, the water flow equations are converted to discrete form using the overlapping cell vertex finite volume method on triangular unstructured mesh, and then, in the second stage, the flow field solution results are used for computing air concentration profiles by a separate post-processor. This post-processor uses experimental relations for computing the inception point characteristics and air concentration distribution profiles along the stepped chute. The computed results of air entrainment into the supercritical skimming flow on stepped spillways have been compared with laboratory experimental measurements.

Key-Words: Air Concentration Distribution, Skimming Flow, Stepped Spillway, Finite Volume Solution, Depth-Averaged Equations

1 Introduction

Over the last two decades, stepped spillways have gained more attention with the development of RCC technique in dam construction. They are also used as an overtopping protection system in embankment dams.

One of the most important advantages of stepped chutes is the reduction of cavitation risk potential because of significant air entrainment and smaller velocities. Another advantage is large amount of energy dissipation in comparison with smooth spillways. Stepped spillways can be easily and economically constructed and attached to the downstream face of RCC dams.

Simulation of flow condition considering the effect s of the air entrainment would help designers of the step spillways to have better understanding about the consequences of the geometric design of this type of hydraulic structures.

The first author successfully developed a finite volume depth averaged flow solver, NASIR[1], which solves depth and velocity fields in dam reservoir as well as over spillway with steep slopes, and then, computes velocity profiles by layered treatment of the flow field, Sabbagh-Yazdi (2007).

In present work the quality of the results of a post processor developed for computation of air concentration in skimming flow is presented. Numerical result of NASIR[2] software, which uses cell vertex finite volume solution of depth average flow equations on unstructured meshes, is used for

[1] Numerical Analyzer for Scientific and Industrial Requirements

processing the air concentration profiles along the spillway as well as in flow depth.

2 Flow Regimes on Stepped Chutes

There are two different flow regimes on stepped chutes: nappe flow and skimming flow. Nappe flow which happens in low discharges consists of a succession of over-falls jumping from one step to another. The steps act as a series of drops plunged one by one by the falling nappes. One part of energy dissipation in the nappe flow regime occurs when the jet breaks in the air. Another part of it is caused by the plunging of nappes on the step surfaces. In this case a hydraulic jump which contributes to energy dissipation might take place.

Skimming flow which happens in large discharges acts as a coherent stream over the outer edges of the steps. These step edges make a pseudo surface over which the flow skims being dissipated by the macro roughness of the steps. The zones formed by the step surfaces and the pseudo bottom contain recirculation vortices which cause part of the energy dissipation in skimming flow regime. The shear transfer from the main stream to the recirculation zone causes the maintenance of the vortices. The exchanges of momentum between the main and the cavity flows results in significant energy dissipation. This paper deals with the skimming flow regime.

A transition flow regime has been observed between the nappe and the skimming flow regimes by Essery and Horner (1978). At the downstream part of the inception point of air entrainment, transition flow exhibits strong splashing and droplet ejections, and air pockets from small to large sizes can be observed.

In high velocity flows on spillways and steep chutes, the turbulent boundary layer reaches the flow surface at the "point of inception", initiating air entrainment into the flow stream.

Observations have shown that there is a developing flow region after the inception point of air entrainment. For some distance in the developing region, there is a region of partially aerated flow, until the air bubbles penetrate to their maximum depth in the water and the flow becomes fully aerated. After the developing region, there is a fully developed aerated flow region where uniform conditions have been obtained.

3 Assumed Flow Condition

The numerical simulation results have been compared with those obtained from the experimental model study on the two-phase skimming flow down a stepped chute conducted at the laboratory of Hydraulics, Hydrology and Glaciology (VAW) of the Swiss Federal Institute of technology (ETH), Zurich. The experiments have been conducted in a prismatic rectangular channel of width 0.5 m and length 5.7 m. The bottom angle $\phi = 30^{\circ}$ and the step height s=46.2mm have been used for comparison. A schema of the laboratory model is shown in Fig.1.

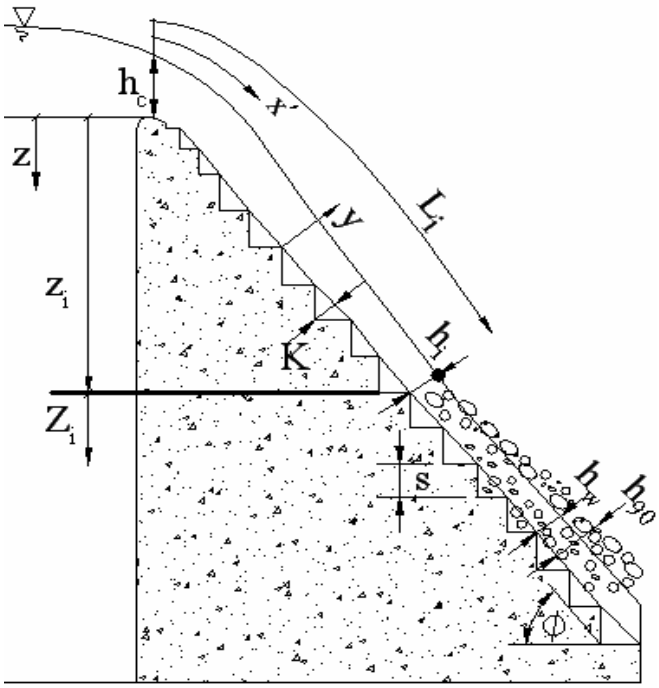

Fig.1: Schematic geometry of the laboratory model and observed flow field, Frizell et al (2000)

In present paper a set of laboratory measurements of above mention researchers are used for the verification of the numerical model which corresponds to skimming flow with unit width discharge of $q=0.0573\ m^2/s$ and Froude Number of $Fr=1.16$.For this case, the laboratory measurements for the inception point the non-dimensional position and water depth are reported $h_i / s = 0.6$ and $z_i / s = 9.5$, respectively. Hence, considering the step height s=46.2mm, the depth at the inception point and the vertical distance measured from the spillway crest to the point of inception are calculated as $h_i=0.028m$ and $z_i=0.439m$, respectively

4 Mathematical Equations

The water phase mathematical equations used in the NASIR[1] flow solver are shallow water equations

[1] Numerical Analyzer for Scientific and Industrial

modified for a coordinate system with an axis normal and two axes(x' and y) parallel to the bed surface according to Sabbagh-Yazdi (2006).

$$\frac{\partial h'}{\partial t}+\frac{\partial (h'u')}{\partial x'}+\frac{\partial (h'v)}{\partial y}=0$$

$$\frac{\partial (h'u')}{\partial t}+\frac{\partial (u'h'u')}{\partial x'}+\frac{\partial (vh'u')}{\partial y}+\frac{\partial}{\partial x'}\left[h'\frac{gh'/\cos\alpha}{2}\right]=gh'\mathrm{Sin}\alpha - gh'S_{fx'}$$

$$\frac{\partial (h'v)}{\partial t}+\frac{\partial (u'h'v)}{\partial x'}+\frac{\partial (vh'v)}{\partial y}+\frac{\partial}{\partial y}\left[h'\frac{gh'/\cos\alpha}{2}\right]=-gh'S_{fy} \quad (1)$$

in which:

$$S_{fx'}=\frac{n^2u'\sqrt{u'^2+v^2}}{h'^{4/3}};S_{fy}=\frac{n^2v\sqrt{u'^2+v^2}}{h'^{4/3}} \quad (2)$$

In these equations x' is the axis tangential to the chute slope and y is the same as the y axis in the global coordinate system; u' and v are the velocity components in x' and y directions, respectively; h' is the flow depth perpendicular to the chute bed surface and g is gravity acceleration; α is the chute angle; $S_{fx'}$ and S_{fy} are the bed surface friction slopes in x' and y directions, respectively and n is Manning's friction coefficient.

In order to use the above described mathematical model for skimming flow over stepped spillway, the effect of the steps has been simulated as bed roughness. For simulating the equivalent bed roughness the following experimental relationship has been used:

$$f_b=[0.5-0.42\sin(2\phi)]\left(\frac{K}{D_{h,w}}\right)^{0.2};19^\circ\le\phi\le55^\circ \quad (3)$$

where $D_{h,w}$ is the hydraulic diameter.

5 Computation of Vertical Velocity Profile

The depth averaged velocity field parallel to the bed surface that can be computed by solving mathematical model described in aforementioned section, may be used for computation of the velocity profile in flow depth. Such a velocity profile can be computed using empirical relations suggested for skimming flow over stepped spillways.

The relation used for defining velocity profiles in flow depth is the Boes and Hager's relation (2003), as follows:

$$\frac{u}{u_{90}}=1.05\left(\frac{y}{y_{90}}\right)^{1/4.3};\ 0.04\le\frac{y}{y_{90}}\le0.80$$

$$\frac{u}{u_{90}}=1;\frac{y}{y_{90}}>0.80 \quad (4)$$

where y_{90} is the characteristic mixture depth with local air concentration of C=0.90 and u_{90} is the mixture surface velocity.

6 Experimental Relations for Air Concentration Distribution

Following experimental relations are used in the post-processor for simulating air entrainment. Frizell et al. (2000) gave a relationship for defining mean air concentration:

$$C_{mean}=0.23+0.017\left(\frac{x-L_i}{y_i}\right)^{0.46} \quad (5)$$

Matos (2000) derived:

$$\begin{cases} C_{mean}=0.210+0.297\exp\left[-0.497\left(\ln\left(\frac{x-L_i}{y_i}\right)-2.972\right)^2\right]; 0<\frac{x-L_i}{y_i}<30 \\ C_{mean}=\left[0.888-\frac{1.065}{\sqrt{\frac{x-L_i}{y_i}}}\right]^2 \quad ;\frac{x-L_i}{y_i}\ge30 \end{cases} \quad (6)$$

where C_{mean} is the mean air concentration, x is the distance from the crest along the chute slope, L_i is the black water length from spillway crest to inception point, and y_i is the flow depth at the point of inception.

Air concentration profiles, compared with an air bubble diffusion model proposed by Chanson (2000), are expressed by:

$$C(y)=1-\tanh^2(K'-\frac{y}{2D'h_{90}}) \quad (7)$$

To define K' and D', the following relationships have been fit to experimental data:

$$K'=0.729C_{mean}^{-0.9932} \quad (8)$$

$$D'=3.4558C_{mean}^{\ 3}-2.2006C_{mean}^{\ 2}+1.1059C_{mean}-0.0117 \quad (9)$$

The following relations have been used for defining the inception point distance from the crest along the chute.

Boes and Minor (2002) derived:

$$L_i=\frac{5.90h_c^{6/5}}{(\sin\phi)^{7/5}s^{1/5}} \quad (9)$$

Chanson (1994) derived:

$$\frac{L_i}{K}=9.719(\sin\phi)^{0.796}F_h^{0.713} \quad (10)$$

Requirements

Chamani (1997) derived:

$$\frac{L_i}{K} = 8.0F_i^{0.858} \quad (11)$$

Matos et al. (2000) derived:

$$\frac{L_i}{K} = 6.289F_s^{0.734} \quad (12)$$

where, $K = s.\cos\phi$, $F_h=q / (g \sin\phi K^3)^{1/2}$, $F_i=q/(g.(s/l).K^3)^{1/2}$, $F_s=q/(g s^3)^{1/2}$, l and s are the step length and height, respectively and ϕ is the chute angle.

The following relations have been used for defining the mixture flow depth at the point of inception.

Boes and Minor (2002) derived:

$$y_i = \frac{0.40s^{0.10}h_c^{0.90}}{(\sin\phi)^{0.30}} \quad (13)$$

Chanson (1994) derived:

$$\frac{y_i}{K} = \frac{0.4034}{(\sin\phi)^{0.04}}F_h^{0.592} \quad (14)$$

7 Numerical Solution of Flow Field

In the first stage, the flow field is numerically solved with NASIR software. This software uses finite volume method for solution of the modified shallow water equations for a coordinate system with an axis tangent to the slope direction (x') and another axis in transversal horizontal direction (y), Sabbagh-Yazdi (2007). The depth and velocity values are depth-averaged values computed on a triangular unstructured mesh using the finite volume method. The equations have been converted to discrete form using the overlapping cell vertex method.

For the numerical modeling of the problem, free slip boundary conditions in wall boundaries are applied by imposing zero normal velocity. At boundary, super critical inflow condition is imposed by enforcing depth and velocity components. The flow depth and velocity values imposed at the inflow boundary are 0.063 m and 0.91 m/s, respectively.The outflow boundary condition is considered free from implementation of any variables.

8 Velocity Profile Computation

As the first post-processing, the depth averaged velocity field parallel to the bed surface which is solved by NASIR software is used to compute the velocity profile in flow depth. The velocity profile is computed using empirical relations suggested for skimming flow over stepped chutes.

Fig. 2 shows normalized velocity (u/u_{90}) in terms of relative flow depth (y/y_{90}). The RMS values for the three stations are almost the same; because steps dissipate energy and the flow keeps an almost constant velocity after a short distance from the crest. So the relationship used for velocity distribution in the numerical simulation creates small RMS values.

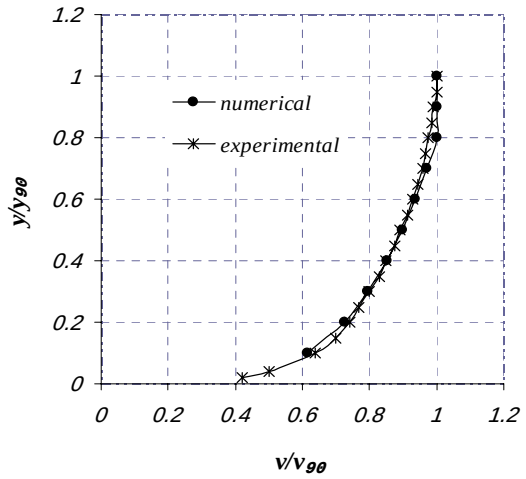

Fig.2: normalized velocity in terms of relative flow depth; comparison between numerical and experimental results, RMS=0.0130

9 Air Concentration Computation

For processing the air concentration all through water flow field, experimental relations have been used for computing the inception point distance from the crest, the flow depth in this section and the depth-averaged air concentration in each point. Then the depth values obtained from the first stage have been modified considering the bulking caused by the entrained air. Finally, the air distribution profiles in flow depth have been obtained from the computed depth-averaged values using experimental relations.

If the non-dimensional vertical distance from the inception point (Fig.1) is defined as $Z_i = (z - z_i)/h_c$, the stations with Z_i=-0.5, Z_i=0.9 and Z_i=41.3 are used for comparison of the computed results of present numerical model with experimental measurements reported for this physical model by Frizell et al (2000). The actual vertical distances of the stations from the spillway crest are listed in the following table.

Table 1: vertical distances of the stations measured from the crest

Station	Z_i	z (m)
1	-0.5	0.43
2	0.9	0.52
3	41.3	3.06

The errors calculated for the relations used for computing the location of the inception point are listed in the table 2 for comparison.

Table 2: errors in location of inception point

relation	error
Boes and Minor (2002)	37.8%
Chanson (1994)	39.4%
Chamani (1997)	2.9%

The errors calculated for the relations used for computing the flow depth at the inception point are listed in the table 3 for comparison.

Table 3: errors in flow depth at the inception point

relation	error
Boes and Minor (2002)	3.6%
Chanson (1994)	3.6%
Matos et al. (2000)	a small value created

In order to choose the best relation for defining mean air concentration, the program has been run for the case of using Chanson's relation for inception point location and flow depth at that section. The root mean square (RMS) of the air concentration profiles in terms of relative flow depth (y/y_{90}) has been compared for the two relations used for defining mean air concentrations. The results are listed in table 4.

Table 4: RMS values of air concentration profiles (using Chanson's relations for inception point)

relation	RMS values of air concentration profiles		
	Zi=-0.5	Zi=0.9	Zi=41.3
Frizell et al. (2000)	0.13	0.06	0.04
Matos et al. (2000)	0.28	0.16	0.15

It can be concluded from table 4 that the relation proposed by Frizell et al. (2000) creates smaller values of RMS when compared to experimental results.

Now the program is run for the case of using Chamani's relation for inception point location, Chanson's relation for flow depth at the point of inception, and Frizell et al.'s relation for mean air concentration. Fig.s 3 to 5 show air concentration (C) in terms of relative flow depth (y/y_{90}) for the three stations mentioned before.

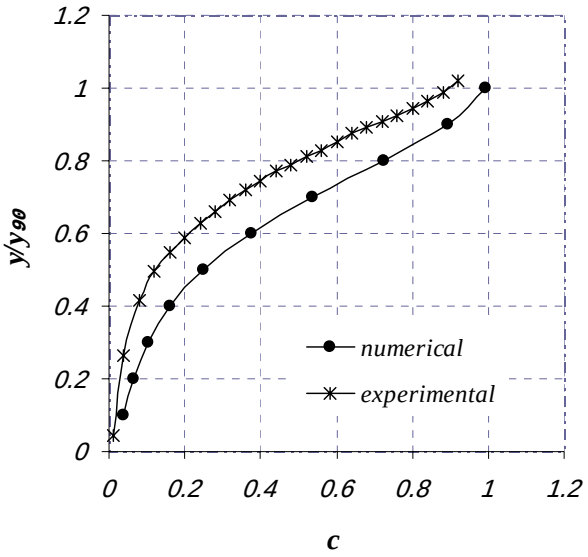

Fig.3: air concentration as function of relative flow depth at station 1; comparison between numerical and experimental results, RMS=0.1375

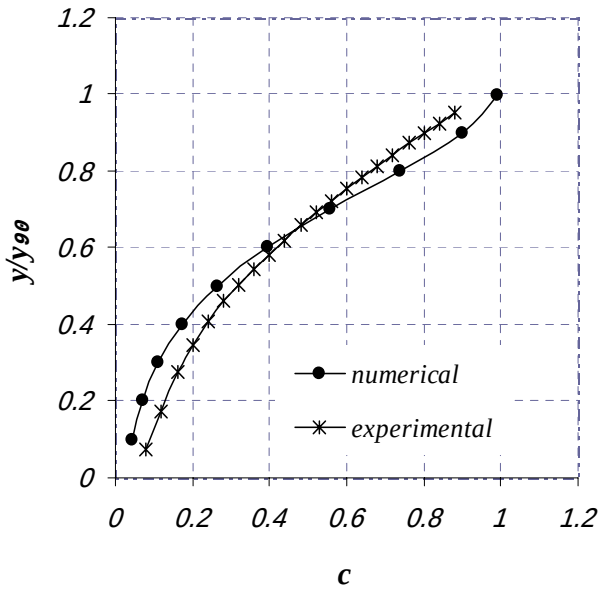

Fig.4: air concentration as function of relative flow depth at station 2; comparison between numerical and experimental results, RMS=0.0602

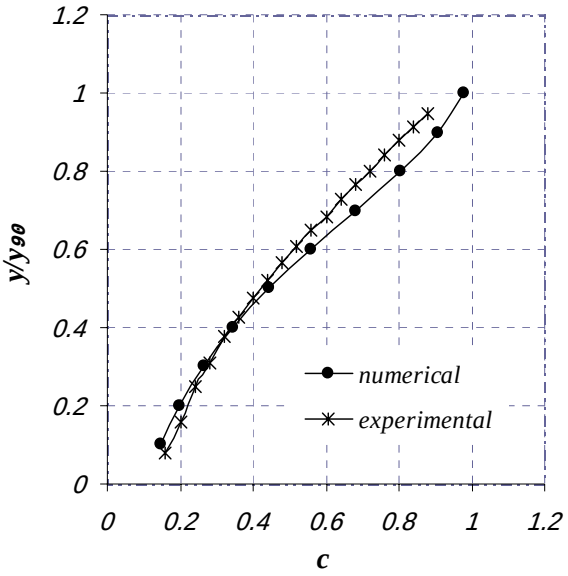

Fig.5: air concentration as function of relative flow depth at station 3; comparison between numerical and experimental results, RMS=0.0479

10 Conclusion

The numerical analysis of skimming flow on stepped spillways has been carried out at two stages. At the first stage, numerical solution of modified shallow water equations for inclined coordinate system is performed using NASIR finite volume flow solver. At the second stage, a post-processor routine is developed, which successfully computes the velocity profile in vertical direction and uses various empirical relations for calculating air concentration profiles.

The comparison of the numerical results with the experimental measurements shows that the following relations for computing air concentration profiles produce better results when they are used as means of post-processing for air entrainment in skimming flow over stepped chutes:

- Relation proposed by Chamani (1997) for defining inception point
- Relations suggested by Boes and Minor (2002) as well as Chanson (1994) for defining flow depth at the inception point
- Relation proposed by Frizell et al. (2000) for defining mean air concentration
- Relation suggested by Chanson (2000) for defining air concentration profiles

References:

[1] James C. S., Ohtsu I., Yasuda Y., Takahasi M., Tatewar P., Ingle N. and Porey D. (2001), Discussion of 'On set of Skimming Flow on Stepped Spillways.' By M. R. Chamani, N. Rajaratnam., *J. Hydraulic Eng*., Vol.127, No.6, pp. 519-525

[2] Dewals B.J., Andre S., Schleiss A.J. and Pirotton M. (2004), Validation of a Quasi-2D Model for Aerated Flows over Mild and Steep Stepped Spillways, *6th International Conference on Hydro-informatics*, pp. 63-70.

[3] Chanson H. (2004), Hydraulics of Stepped Chutes: The Transition fFow, *J. Hydraulic Res*., Vol.42, No.1, pp. 43-54

[4] Chanson H. and Toombes L., (2001), Experimental Investigation of Air Entrainment in Transition and Skimming Flows Down a Stepped Chute, Research Report No. CE 158,

[5] Chamani M.R. (1997), Skimming Flow in a large Model of a Stepped Spillway, Thesis for the Degree of Doctor of Philosophy in Water Resources Engineering,

[6] Rajaratnam N. (1990), Skimming Flow in Stepped Spillways., *J. Hydraulic Eng*., Vol.116, No.4, pp. 587-591.

[7] Khatsuria R.M. (2005), Hydraulics of Spillways and Energy Dissipaters", pp. 95-127

[8] M. Boes, H. Hager, Hydraulic Design of Stepped Spillways, *J. Hydraulic Eng*., Vol.129, No.9, 2003, pp. 671-679

[9] Boes M. and Hager H. (2003), Two-Phase Flow Characteristics of Stepped Spillways, *J. Hydraulic Eng.*, Vol.129, No.9, pp. 671-679.

[10] Sabbagh-Yazdi, S.R. (2006), Spillway Flow Modeling by Finite Volume Solution of Slopping Depth Averaged Equations on Triangular Mesh; Application to KAROUN-4 Spillway, *10th WSEAS International Conference on Applied Mathematics*, Dallas (Texas), USA

[11] Sabbagh-Yazdi, S.R., N.E. Mastorakis and Zounemat M. (2007), Velocity Profile over Spillway by Finite Volume Solution of Slopping Depth Averaged Flow, 2nd IASME/WSEAS *International Conference on Continuum Mechanics*, Slovenia (to be appeared in proceeding CD)

[12] Yoon T.H. and Kang S.K. (2004), Finite Volume Model *for* Two-Dimensional Shallow Water Flows on Unstructured Grids, *J. Hydraulic Eng*., Vol. 130, No.7, pp. 678-688